

Hybrid composites of ABS with carbonaceous fillers for electromagnetic shielding applications

Débora P. Schmitz,¹ Tamara I. Silva,² Sílvia D. A. S. Ramoa,¹ Guilherme M. O. Barra ¹,
Alessandro Pegoretti,³ Bluma G. Soares ²

¹Departamento de Engenharia Mecânica, Universidade Federal de Santa Catarina, Florianópolis, Santa Catarina, Brazil

²Departamento de Engenharia Metalúrgica e de Materiais, Universidade Federal do Rio de Janeiro, Rio de Janeiro, Brazil

³Department of Industrial Engineering and INSTM Research Unit, University of Trento, Trento, Italy

Correspondence to: G. M. O. Barra (E-mail: g.barra@ufsc.br)

ABSTRACT: This work evaluates the influence of two types of carbonaceous fillers, carbon black (CB) and carbon nanotubes (CNTs), on the electrical, electromagnetic, and rheological properties of composites based on poly(acrylonitrile-*co*-butadiene-*co*-styrene) (ABS) prepared by the melt mixing. Electrical conductivity, electromagnetic shielding efficiency (EMI SE) in the X-band frequency range (8–12.4 GHz), and melt flow index (MFI) results showed that ABS/CNT composites exhibit higher electrical conductivity and EMI SE, but lower MFI when compared to ABS/CB composites. The electrical conductivity of the binary composites showed an increase of around 16 orders of magnitude, when compared to neat ABS, for both fillers. Binary composites with 5 and 15 wt % of filler showed an EMI SE of, respectively, –44 and –83 dB for ABS/CNT, and –9 and –34 dB for ABS/CB. MFI for binary composites with 5 wt % were 15.45 g/10 min and 0.55 g/10 min for CB and CNT, respectively. Hybrid composites ABS/CNT/CB with 3 wt % total filler and fraction 50:50 and 75:25 showed good correlation between EMI SE and MFI. © 2018 Wiley Periodicals, Inc. *J. Appl. Polym. Sci.* **2018**, *135*, 46546.

KEYWORDS: dielectric properties; structure–property relationships; thermoplastics

Received 30 October 2017; accepted 4 March 2018

DOI: 10.1002/app.46546

INTRODUCTION

Electromagnetic wave emission has increased due to the proliferation of personal electronics, such as smartphones, tablets, and personal computers. These emissions have the potential to interfere on other electronic devices functions and may also be harmful to living organism as well as human health. For this reason, great effort has been made to develop materials with improved electromagnetic interference (EMI) shielding efficiency (SE) to prevent such undesirable effects.^{1–6}

Electrically conducting polymer composite (CPCs) are a good alternative material, since they present low weight, corrosion resistance, easy processing associated with electrical and dielectric properties suitable to prevent electrostatic discharge, disturbance, and mutual interference among electronic systems. CPCs can be obtained by combining polymer matrices with electrically conductive fillers, such as metallic powders, carbonaceous particles or additives such as intrinsically conductive polymers, among others. Many interesting research studies focusing on the CPCs were carried out in order to produce shielding materials with improved properties and, some of the most interesting

results have been obtained by using carbonaceous nanofillers, such as carbon nanotubes (CNTs),^{1,2,4} expanded graphite,³ carbon black (CB),^{1,3,4} carbon fiber (CF),⁴ and graphene (GE).² Carbonaceous nanofillers represent a good choice as conductive fillers due to their low specific weight, good intrinsic electrical conductivity, and good interfacial adhesion. Those properties allow the production of CPCs with desirable mechanical properties, electrical conductivity, and EMI SE.

A major goal for fabrication of CPCs is to achieve the highest EMI SE, electrical conductivity, and dielectric properties at the lowest filler content. Higher amounts of filler tend to produce composites with reduced mechanical and rheological properties. There are several characteristics of both matrix and filler that can influence the electrical, rheological, and electromagnetic properties of CPCs, such as filler aspect ratio, matrix–filler, and filler–filler interactions and processing parameters.^{7–9}

One very interesting strategy for reducing the filler content of CPCs is by incorporating two or more conductive fillers into insulating polymer matrix.^{2,5,7,10,11} The incorporation of different fillers in the same matrix (hybrid systems) may improve the composite properties if a synergistic effect is reached.^{2,12–15}

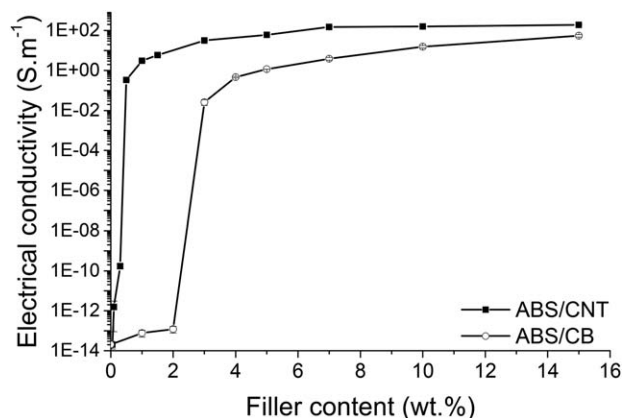


Figure 1. Electrical conductivity of ABS/CNT and ABS/CB as function of filler content.

Kuester *et al.*² demonstrated a synergistic effect on the EMI SE of poly(styrene-*b*-ethylene-*ran*-butylene-*b*-styrene) (SEBS) filled with CNT and GE nanoplatelets (GnP), where the EMI SE values for the hybrid composites were significantly higher than those observed for the nanocomposites containing the individual fillers. With a total amount of 10 wt % the single filler composites showed EMI SE of 6.37 dB for SEBS/GnP, and 20.78 dB for SEBS/CNT, while the hybrid systems SEBS/GnP/CNT with component fraction of 2:8 (GnP:CNT) presented a SE of 23.30 dB. Sharma *et al.*¹³ studied the synergistic effect of adding 1 wt % of multi-walled carbon nanotube (MWCNT) in GE/ABS composites. The addition of MWCNT in the GE/ABS composites resulted in higher increase on SE than what was expected by the numerical sum of the values obtained by the individual fillers.

Another very important characteristic to improve EMI SE is a proper selection of the polymer matrix.¹⁶ Among insulating polymer matrices, the thermoplastic terpolymer poly(acrylonitrile-*co*-butadiene-*co*-styrene) (ABS) offers interesting possibilities to produce CPCs because of its high toughness, good thermal stability, low coefficient of thermal expansion, high resistance to attacks chemical and high durability. Moreover, ABS exhibits a good processability and a reduced cost when compared to other polymers with similar properties, which allows its application in different technological areas.

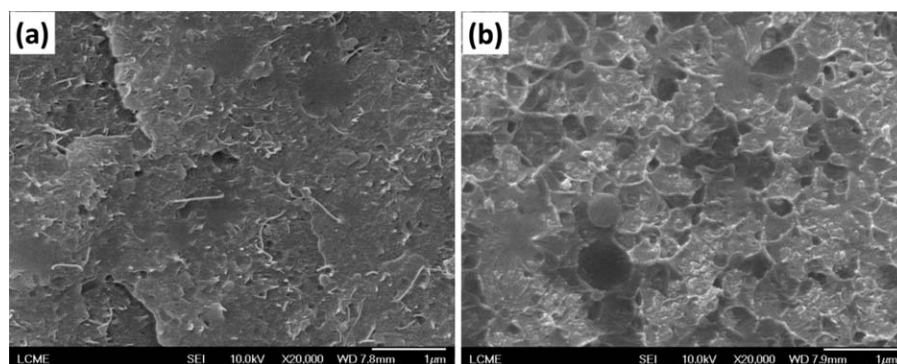


Figure 2. FEG-SEM micrographs of composites with the two different filler: (a) ABS/CNT 5 wt % and (b) ABS/CB 5 wt %. Magnification of 20,000 \times .

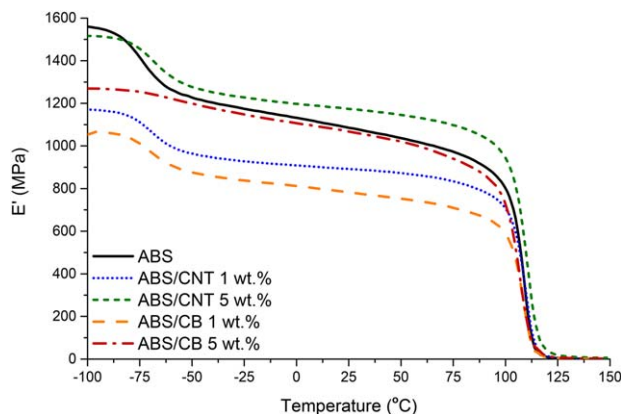


Figure 3. Storage modulus (E') versus temperature at 1 Hz of ABS/CNT and ABS/CB for different filler concentrations. [Color figure can be viewed at wileyonlinelibrary.com]

Jyoti *et al.*¹⁷ analyzed the electrical properties of MWCNT/ABS composites with different MWCNT content. The percolation threshold obtained for the composites was 1 wt % and EMI SE increased from 1.26 dB for neat ABS (ABS0) to 32 dB for MWCNT/ABS with 10 wt % of filler (ABS10). Al-Saleh *et al.*⁴ compared the electrical and electromagnetic properties of ABS composites based on three different carbonaceous fillers (CB, CNF, and CNT) prepared by solution processing. CNT/ABS showed smaller percolation threshold and higher EMI SE than CNF/ABS and CB/ABS. Al-Saleh and Saadeh¹⁸ also studied the EMI SE evolution of CNT:CF/ABS and CNT:CB/ABS hybrid composites, prepared by solution processing, with same total filler amount (5 wt %) but different component fractions. For all the analyzed systems the SE increased with increasing CNT content and no synergistic effect was found. However, the CNT:CB/ABS composites with a 4:1 fraction showed very similar EMI SE value to the 5 wt % CNT/ABS composite, which allows the production of composites with the desired SE but using less CNT. Furthermore, the CNT:CB showed better SE than CNT:CF, mostly because of the morphology obtained.

Although there are some studies on electrical and electromagnetic applications of CPC based on ABS with different types of fillers, the composites preparation vary among them and the most commonly used is solution processing. The attention to

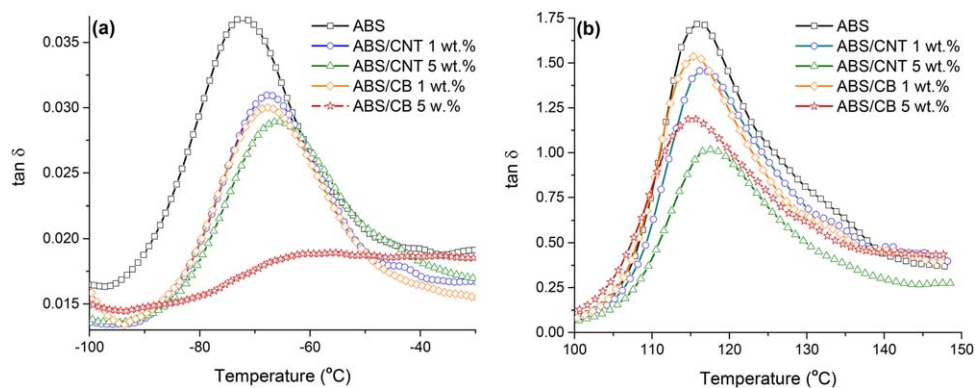


Figure 4. $\tan \delta$ versus temperature at 1 Hz of different composites for (a) butadiene phase and the (b) SAN phase. [Color figure can be viewed at wileyonlinelibrary.com]

processing conditions is not only important due to its influence on the final properties of the composites, but also because it may influence on the adoption of the system by the industry. Melt mixing is an industrially relevant process to produce CPCs because it is clean (it does not use solvents), cheap, and can be easily scaled up. Moreover, to the extent of our knowledge, there are no studies reporting the influence of CNT and CB incorporation on the processability and EMI-SE of CPCs based on ABS obtained by melt mixing.

Based on the above considerations, the aim of this work is to produce electrically conductive composites comprising of CB and CNTs filler and a ABS matrix, by melt mixing process, and investigate their rheological behavior (melt flow index, MFI), electrical conductivity, and EMI SE. The study also intends to investigate the microstructure of the obtained CPCs in terms of distribution of nanofillers in the matrix. Finally, this work aims to find the best content and mixing ratio between the fillers (CNT and CB) to attain a hybrid composite with desirable EMI SE (around 20 dB for commercial use) and MFI to be easily processed.

EXPERIMENTAL

Materials

ABS granules grade Cyclic Resin MG47 with a specific gravity of 1.04 and MFI (220 °C/10 kgf) of 18 g/10 min were provided by Sabic (Brazil). The MWCNTs grade Nanocyl NC7000 were provided by Nanocyl S.A (Belgium) with an average diameter of 9.5 nm, an average length of 1.5 μm , a carbon purity of 90%, a surface area between 250 and 300 $\text{m}^2 \text{g}^{-1}$, and electrical conductivity of 10^4 S m^{-1} . The CB particles, grade Printex XE 2-B, with an average particle size of 30 nm, a surface area of 1000 $\text{m}^2 \text{g}^{-1}$, and electrical conductivity of 210 S m^{-1} was purchased from Orion Engineered Carbons (Belpre, Ohio) (USA).

Composites and Sample Preparation

Binary composites of ABS with different amounts of MWCNT (varying from 0.05 to 15 wt %) and CB (varying from 1 to 15 wt %) were prepared by melt mixing. First, all the components were dried overnight at 60 °C to remove the absorbed moisture. Then, the materials were mixed in a Thermo Haake PolyLab Rheomix 600p internal mixer at 230 °C and at a rotor speed of 60 rpm for 15 min (2 min to melt the neat ABS and 13 min for complete mixing). The hybrid composites of ABS/CNT/CB were

prepared following the similar procedure, but firstly the two filler were manually mixed and then were added to the fused matrix. The total amount of filler incorporated was 1, 3, and 5 wt % and the fraction of each filler component (CNT:CB) in the composites changed between 25:75, 50:50, and 75:25.

After melt mixing, samples were manufactured by thermo-compression molding in a hot-plate hydraulic press at 230 °C for 5 min under different pressures depending on the target sample's geometry, to insure the complete filling of the mold and the least amount of voids in the sample.

Methodology

Electron Microscopy. Morphology and filler dispersion were analyzed by field emission gun scanning electron microscopy (FEG-SEM), using a Jeol model JSM-6390LV microscope at an applied tension of 10 kV, and by transmission electron microscopy (TEM), using Joel model JEM-2100 at applied tension of 80 kV. The FE-SEM samples were broken in a brittle manner after cooling in liquid nitrogen, and the obtained fracture surfaces were sputtered with a gold layer. The TEM samples were sectioned by ultramicrotomy, section with thickness of approximately 70 nm, and collected in a copper mesh grid.

Electrical Conductivity. Electrical conductivity is the reciprocal of electrical resistivity and it may be defined as the easiness of an electron to move through a material, it is the capacity a material has to conduct electrical current when voltage is applied. The volume electrical conductivity measurements were made at room temperature by using the four-probe standard

Table I. Activation Energy of the ABS/CNT and ABS/CB Composites Temperature Transition (T_g) for the Butadiene and SAN Phases

	Filler amount (wt %)	Activation energy (kJ mol^{-1})	
		Butadiene	SAN
Neat ABS		159 \pm 12	547 \pm 31
CNT	1	175 \pm 23	550 \pm 65
	5	192 \pm 27	507 \pm 66
CB	1	162 \pm 23	490 \pm 27
	5	122 \pm 30	497 \pm 13

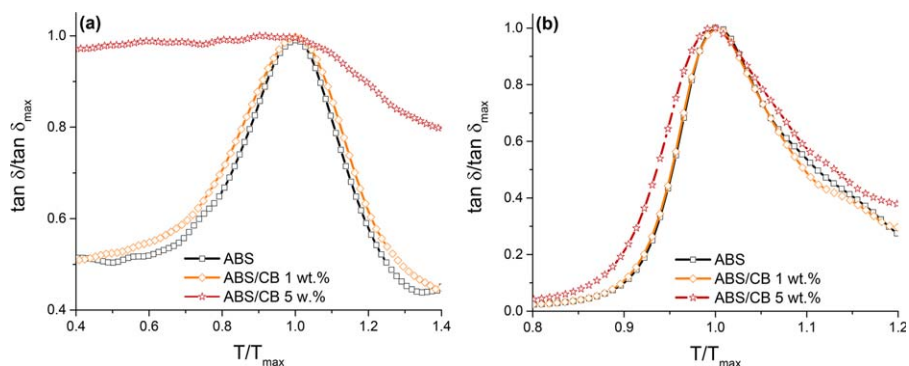


Figure 5. Normalized curve of $\tan \delta / \tan \delta_{max}$ as a function of T/T_{max} at 1 Hz for (a) butadiene and (b) SAN phase in neat ABS and ABS/CB composites with 1 and 5 wt % filler content. [Color figure can be viewed at wileyonlinelibrary.com]

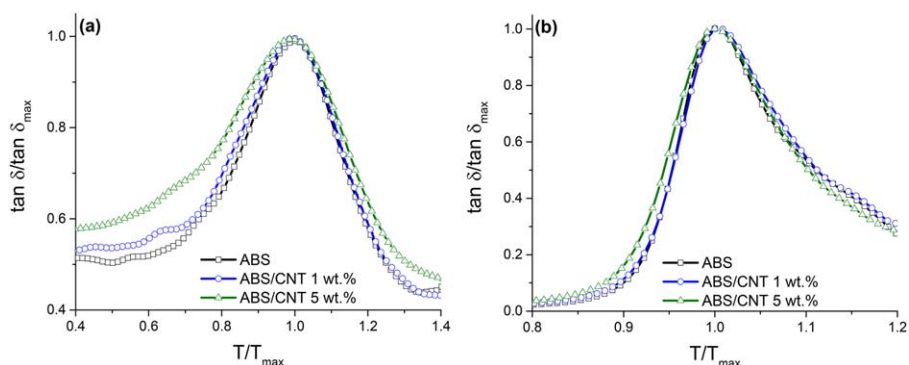


Figure 6. Normalized curve of $\tan \delta / \tan \delta_{max}$ as a function of T/T_{max} at 1 Hz for (a) butadiene and (b) SAN phase in neat ABS and ABS/CNT composites with 1 and 5 wt % filler content. [Color figure can be viewed at wileyonlinelibrary.com]

method for high-conductivity samples and the two-probe method for high-resistivity samples.

The four-probe method was performed using a Keithley 6220 current source to apply the current and a Keithley Model 6517A electrometer to measure the voltage. The four-probes (gold plated with diameter of 1 mm) are arranged in a series form, with 1 mm distance between them. To calculate the electrical conductivity, eq. (1) was used.

$$\sigma = \frac{I}{V} \frac{1 \ln 2}{d \pi} \quad (1)$$

where σ is the volume electrical conductivity ($S \text{ m}^{-1}$), I is the applied current (A), V is the measured voltage (V), and d is the sample thickness (m).

For high-resistivity samples, the volume conductivity measurements were carried out using a Keithley 6517A electrometer

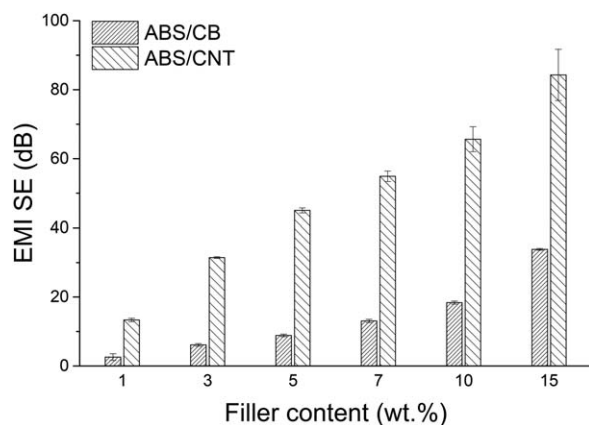


Figure 7. EMI SE of ABS/CNT and ABS/CB samples as a function of filler content.

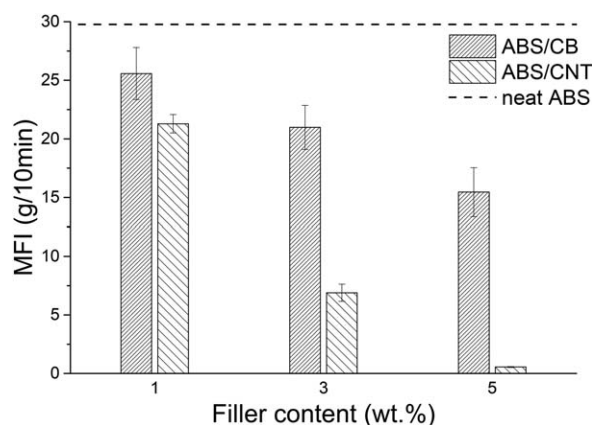


Figure 8. MFI of binary composites as a function of filler content. The dotted line represents the MFI of neat ABS.

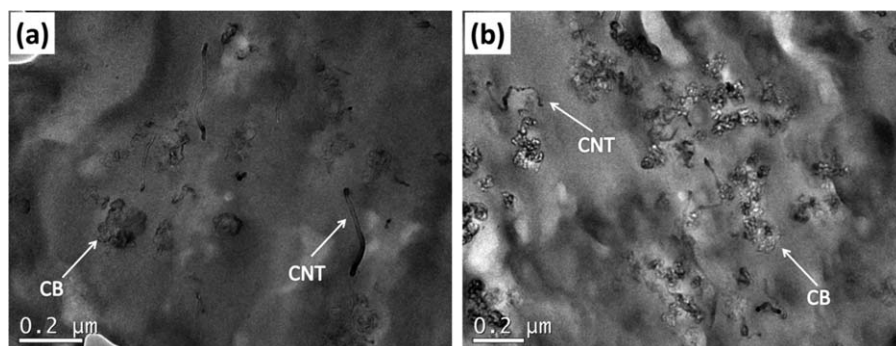


Figure 9. TEM images of hybrid composites (25:75) containing (a) 1 wt % and (b) 3 wt % of CNT:CB.

connected to a Keithley 8009 test fixture. Equation (2) was used to calculate the samples' electrical resistivity.

$$\rho = \frac{K_v V}{w I} \quad (2)$$

where, ρ is the samples' electrical resistivity (Ω cm), K_v is a constant related to the electrode geometry (cm^2), w is the samples' thickness (cm), V is the applied voltage (V), and I is the measured electrical current (A).

Since electrical conductivity is the reciprocal of electrical resistivity, the values can be obtained using eq. (3).

$$\sigma = \frac{1}{\rho} \quad (3)$$

The tested specimens had dimensions of 90 mm \times 90 mm \times 0.3 mm.

Dynamic Mechanical Thermal Analysis. Dynamic mechanical thermal analysis (DMTA) tests were carried out in a Netzsch 242 E Artemis device under single cantilever mode with free bending length of 16 mm. The analysis was in multi-frequency dynamic mode, with four different frequencies: 1, 2.5, 5, and 10 Hz. The temperature ranged from -100 to 150 $^{\circ}\text{C}$, at a heating rate of 3 $^{\circ}\text{C min}^{-1}$, with applied strain amplitude of 20 μm . The storage modulus (E') and the loss tangent ($\tan \delta$) as a function of temperature were acquired for each frequency.

Storage modulus is proportional to the amount of energy stored when a cyclic load is applied, it is a measure of the materials elastic properties, and defines the stiffness of a viscoelastic material. E' can be calculated following eq. (4).

$$E' = \frac{\sigma_a}{\varepsilon_a} \cos \delta \quad (4)$$

where σ_a is the stress amplitude (Pa), ε_a is the strain amplitude, and δ is the phase angle between applied stress and strain (rad).

Three specimens were prepared with thickness of 3 mm, width of 12 mm, and length of 30 mm.

Melt Flow Index. MFI represents the flow rate of a polymer as a function of a pre-determined amount of time, usually expressed in grams by 10 min (g/10 min).

The MFI was measured at a temperature of 230 $^{\circ}\text{C}$ under an applied weight of 10 g using a CEAST model 7026.000 device.

EMI SE. The EMI SE analysis was carried out in the X-band frequency range (8–12.4 GHz) using an N5230C Agilent PNA-L network analyzer (Agilent Technology PNA series) connected to a rectangular waveguide, working as the sample holder. The specimens used had dimension of 50 mm \times 50 mm \times 2 mm. EMI SE is measured by recording the S -parameters, which includes the intensities of incident wave S_{11} (or S_{22}) and the transmitted wave S_{12} (or S_{21}), according to eq. (5).

$$\text{EMI SE} = 10 \log \frac{1}{|S_{12}|^2} = 10 \log \frac{1}{|S_{21}|^2} \quad (5)$$

RESULTS AND DISCUSSION

Binary Composites

Initially, to understand the effects of CNT and CB in the ABS matrix, binary composites were produced. As expected, the electrical conductivity of the binary composites, increased with the filler content. Figure 1 shows the evolution of the electrical conductivity of ABS/CNT and ABS/CB as a function of the filler content.

The abrupt increase in conductivity can be explained by the electrical percolation theory. Electrical percolation threshold is the critical fraction of additive necessary to create conductive pathways inside a material, and is generally modeled according to a power law equation [eq. (6)].

$$\sigma = \sigma_0 (\varphi - \varphi_c)^t \quad (6)$$

where σ is the composites electrical conductivity (S m^{-1}), σ_0 is a constant (S m^{-1}), φ is the fillers weight fraction (wt %), φ_c is the filler weight fraction at the percolation threshold (wt %), and t the conductivity, or critical, exponent. The conductivity exponent t is related to the number of contacts between the filler particles at the percolation as well as the form of the conductive network, i.e., one-, two-, or three-dimensional systems, and the particles dispersion.

The ABS/CNT composites have an electrical percolation threshold of 0.3 wt % and t of 2.4 whereas for the ABS/CB composite the threshold value is at 3 wt % with a t of 2.2. For both systems the critical exponent values are higher than 2 (value related to a three-dimensional system) which implies multiple percolation or tunneling. The electrical conductivity increased by about 16 orders of magnitude when compared to neat ABS, from 10^{-14} S m^{-1} up to about 100 S m^{-1} at 15 wt %.

The observed difference in electrical percolation is most likely linked to the fact that CNT presents higher aspect ratio and intrinsic conductivity than CB.^{1,4,19,20} The same conclusion was reported by Al-Saleh *et al.*⁴ by comparing the electrical properties of three different fillers such as CNT, CF, and CB incorporated in an ABS matrix. The authors reported electrical percolation thresholds of 0.5 wt % for CNT/ABS, between 4 and 5 wt % for CB/ABS, and between 1.25 and 1.5 wt % for CF/ABS.

However, in the present study ABS/CNT composites showed not only a smaller percolation threshold when compared to ABS/CB, but also when compared to other systems.^{1,20–23} For example, Socher *et al.*²³ found the electrical percolation threshold of polyamide 12/CNT composites (Nanocyl NC7000-PA12) to be 0.9 wt %, while Kuester *et al.*²¹ obtained a percolation threshold of 1 wt % for poly(styrene-*b*-ethylene-*ran*-butylene-*b*-styrene) filled with CNTs. A percolation threshold value of 0.7 and 0.9 wt % was attained by Menzer *et al.*²⁰ for composites based on maleic anhydride modified isotactic polypropylene with MWNTC as received and ball milled, respectively. The low percolation threshold value observed for ABS/CNT composites could be related to a selective distribution of the CNT in the ABS matrix. In fact, some studies have showed that by creating a preferential localization for the filler in the polymeric matrix it is possible to decrease the percolation threshold, since the concentration of conductive filler is increasing at local level thus creating conductive pathways.²⁴

Since ABS presents morphology similar to polymeric blends this selective distribution is possible, as long as the CNT shows better affinity to one of its domain than the other. Al-Saleh and Sundararaj²⁵ claim that CNTs are preferably localized in the SAN phase rather than the butadiene phase, due to a thermodynamic affinity. However, the microstructure of the studied composites in the present work (Figure 2) shows a homogeneous distribution of both fillers in the matrix, and it is therefore difficult to confirm if there is any selective distribution.

To determine if one of the reasons for the low percolation threshold showed by the ABS/CNT is truly due to a selective distribution, the composites activation energy (E_a) was calculated and compared to the value for neat ABS. E_a is associated with polymer transitions, such as glass transition, and represents the amount of energy necessary for the chains to move and the transition occur, which can be associated with the interaction between the phases of the polymeric matrix and the fillers.^{26–28} One method to calculate E_a is by taking the glass transition temperature (T_g) at different frequencies from DMA analysis and applying the values corresponding to the maximum temperature of the loss tangent ($\tan \delta$), to an Arrhenius plot. The Arrhenius equation is shown below [eq. (7)].

$$\ln(f) = \frac{E_a}{RT_g} \quad (7)$$

where f is the applied frequency (Hz), E_a is the activation energy (kJ mol^{-1}), T_g is the glass transition temperature (K), and R is the gas constant ($\text{kJ K}^{-1} \text{mol}^{-1}$). The Arrhenius plot is the $\ln f$ versus the inverse of the temperature ($1/T$). The

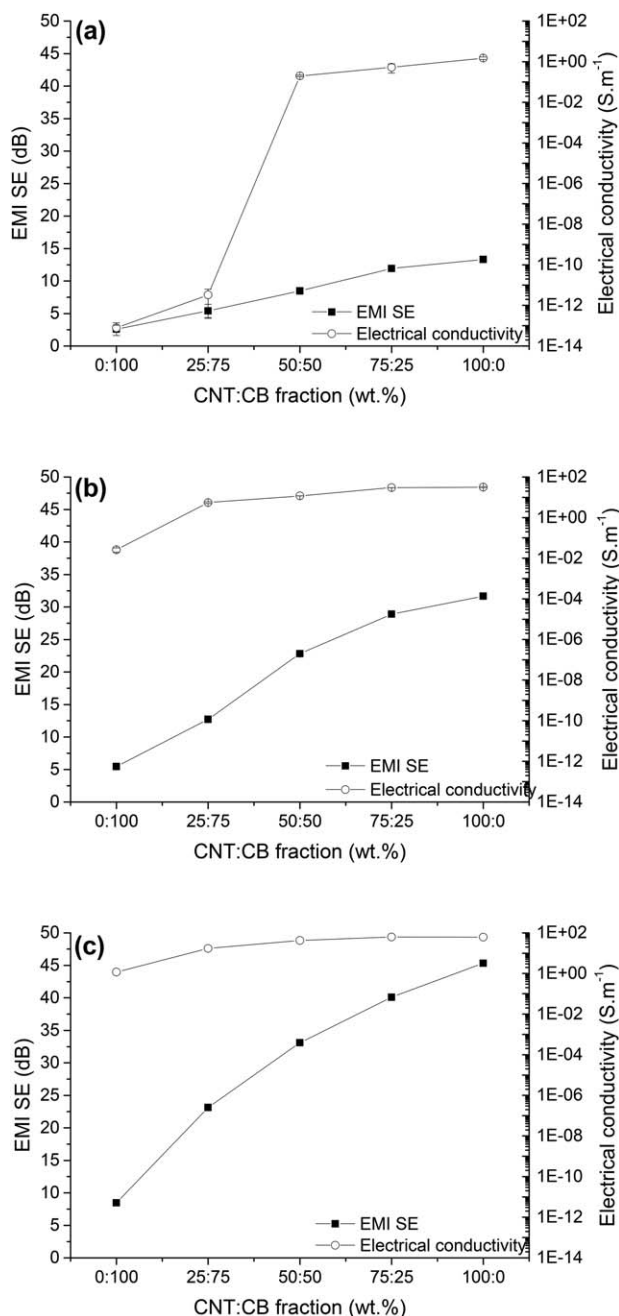


Figure 10. EMI SE and electrical conductivity of composites as a function of each filler fraction. The hybrid composites have a total filler content of (a) 1 wt %, (b) 3 wt %, and (c) 5 wt %.

dependence of the storage modulus with temperature (taken at a frequency of 1 Hz) for the ABS-based composites containing different filler content is illustrated in Figure 3.

Two transitions drops can be observed for all composites, one around -75°C which is related to the glass transition of the butadiene phase, and one around 115°C that corresponds to the glass transition of the SAN phase. As it can be seen, E' values for the composites are lower than those of neat ABS for very low temperatures, around -100°C , and remain lower for all the composites with the exception of the sample ABS/CNT

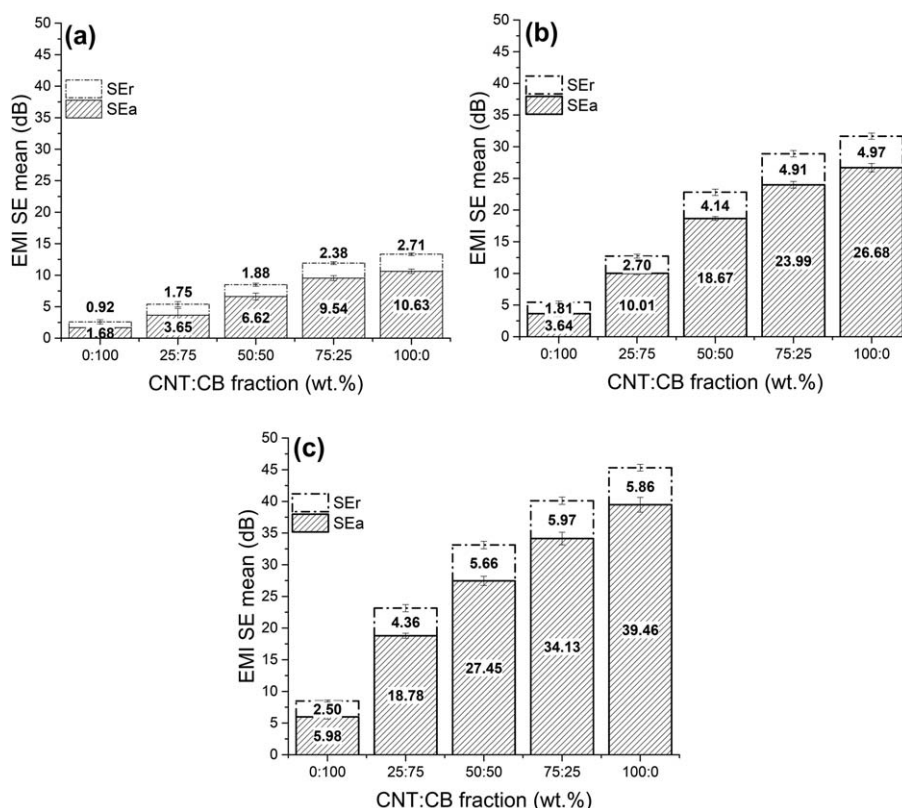


Figure 11. EMI SE mechanisms of composites as a function of filler fraction with total filler content of (a) 1 wt %, (b) 3 wt %, and (c) 5 wt %.

5 wt %. In fact, E' values for ABS/CNT 5 wt % becomes higher than the neat ABS for temperatures above -80°C . The decrease in storage modulus may be related to a plasticizer effect caused by the rise in free volume when the fillers are incorporated, due to a weak filler–matrix interaction. However, with the increase in filler content this volume diminishes, the particles start to have more contact with the polymeric chains and the modulus increase. With the increase in filler content, the reinforcing effect of the filler becomes important, thus contributing for an increase in modulus. This behavior is significant after the glass transition of the butadiene (PBD) phase.

Figure 4 shows the curves of loss tangent ($\tan \delta$) versus temperature for ABS and the composites with 1 and 5 wt % of each filler. The glass transition (T_g) temperature for the butadiene [Figure 4(a)] and SAN phase [Figure 4(b)], for the neat ABS, are -73 and 116°C , respectively. For the composites, the T_g for the butadiene phase has a slight increase in temperature while the ones for the SAN phase remains fairly similar to the neat matrix. On the other hand, the intensity of the peaks reduced considerably with increase in filler content, which can be related to the decrease in flexibility of the polymer molecules due to the incorporation of more rigid fillers. The most pronounced change can be seen for the butadiene phase peak of ABS/CB 5 wt % [Figure 4(a)], indicating a certain preference of CB particles for this phase.

The frequencies used for the DMA analysis were 1, 2.5, 5, and 10 Hz, and the values of E_a obtained are displayed in Table I. Because of the significant variance between the samples for each

composition, it cannot be said that the E_a differ among them, since the changes observed are inside the calculated standard deviation.

Filler distribution can also be estimated by normalizing the curve of loss tangent versus temperature, by dividing the whole curve by the maximum value of $\tan \delta$ ($\tan \delta_{\max}$) and its correspondent maximum temperature (T_{\max}), and analyzing the widening of the normalized plot for the different composites compositions. A broadening in the curve $\tan \delta / \tan \delta_{\max}$ versus T/T_{\max} implies the presence of filler in the respective phase.^{26,27}

The normalized plots, shown in Figures 5 and 6, illustrate the curves for ABS/CB and ABS/CNT, respectively. For ABS/CB it can be seen a widening in the normalized curve with the increase of filler content for both phases. Besides that, it is possible to notice that the effect of the filler is much larger in the butadiene phase than in the SAN phase. Moreover, $\tan \delta$ peak of the butadiene phase is almost not visible for the composite with 5 wt % of CB, indicating a very rigid phase due to, most likely, the presence of a high amount of filler, which agrees with the results initially seen at the T_g peaks. On the other hand, for ABS/CNT the widening of the butadiene phase peak is less pronounced and very little changes can be seen for the SAN phase. These results show that, for the studied concentrations, the fillers are present in both phases but are more pronounced in the butadiene phase.^{26–28}

Figure 7 displays the EMI SE as a function of filler amount for both composites. EMI SE is a property that depends specially on the composites electrical conductivity, filler amount, and

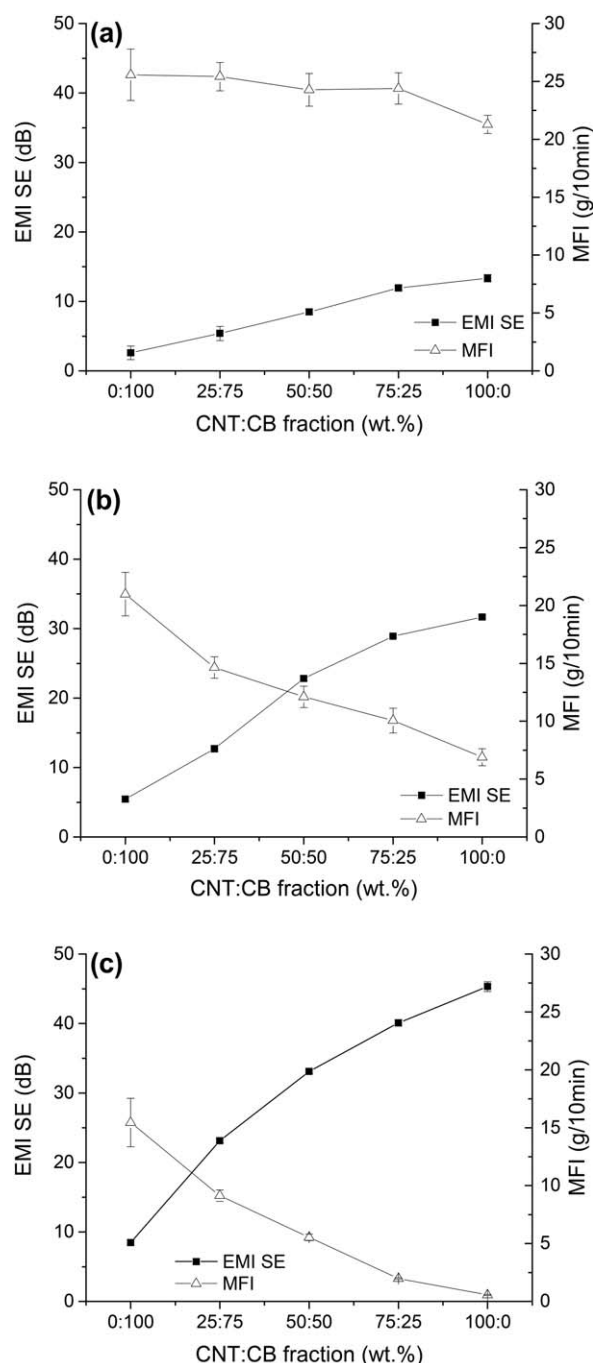


Figure 12. EMI SE and MFI of composites as a function of filler fraction with total filler content of (a) 1 wt %, (b) 3 wt %, and (c) 5 wt %.

distribution, and the sample thickness. Since the thickness of the samples was kept constant for all compositions, the observed changes can be attributed to the other parameters. Both composites, ABS/CNT and ABS/CB, exhibited an increase on EMI SE with increasing filler concentration. Additionally, the EMI SE of composites based on CNT are always higher when compared to the CB based, and the change in value, related to the filler content, is also more accentuated for ABS/CNT. CNT-based composites present a level of shielding at least twice as high as the one measured on CB-based composites, which can

be assigned to the higher aspect ratio of CNT that allows the creation of a tridimensional network of conductive fillers with a smaller amount of particles, these results are corroborated by the attained critical exponents (t) values, where the CNT value is superior to CB, which shows a higher tendency for the ABS/CNT to conduct by means of tunneling.

For commercial usage, the desirable value of shielding is at least 20 dB, which in attenuation percentage corresponds to an attenuation of 99%.²¹ The ABS/CNT with a filler content of 3 wt % already presented a EMI SE of 31.45 dB which raised up to 84.29 dB for 15 wt %. On the other hand, to get to the same minimal desirable value, a CB amount of about 10 to 15 wt % was required to obtain EMI SE values of 18.52 and 33.83 dB, respectively.

Although the growth of EMI SE is a desirable target, the rise in filler content induces a negative increase of material viscosity at the processing temperature, as documented by the decrease of MFI.

For all the composites, the addition of filler resulted in a decrease in MFI (Figure 8), however the ones based on CB presented higher value of MFI and smaller decrease with the addition of filler (from 25.58 g/10 min for 1 wt % to 15.45 g/10 min for 5 wt %). In comparison, the CNT-based composites show a higher dependence of the viscosity on the filler content with MFI values decreasing from 21.29 g/10 min (at 1 wt % of CNT) to 0.55 g/10 min (at 5 wt % of CNT). It is important to emphasize that ABS/CNT with amounts of filler higher than 5 wt % were too viscous to be analyzed, due probably to the formation of a rigid filler network that impairs the polymer's chain movements, at the tested temperature of 230 °C, because of the high amount of filler.

Hybrid Composites of ABS/CNT.CB

In order to keep the desirable electrical conductivity and EMI SE, but avoid the decrease in MFI, hybrid composites of ABS/CNT.CB were manufactured. The intention was to reduce the amount of CNT needed to obtain good EMI SE yet maintain a high MFI. Hybrid composites with 1, 3, and 5 wt % were prepared and the influence of each component on the electrical conductivity, EMI SE, and MFI was measured by changing the weight fraction amount of the different fillers. Figure 9 shows the TEM images of ABS/CNT.CB hybrid composites. Through visual analysis of the TEM images it is possible to infer that the CNT fibers are presented well dispersed and distributed in the polymer matrix, i.e., they appear as single fibers (good dispersion) throughout the whole image (good distribution). On the other hand, the CB particles appear as well distributed small agglomerates. No large agglomeration is visible, which corroborate the electrical conductivity results for the small percolation threshold, and small agglomeration of the CB particles were expected, since this is related to their high structured morphology.

Figure 10 displays the correlation between EMI SE and electrical conductivity as a function of the fraction of each filler in the composite, for [Figure 10(a)] 1 wt %, [Figure 10(b)] 3 wt %, and [Figure 10(c)] 5 wt % total amount of filler. All

Table II. ABS/CNT:CB Hybrid Composites Summarized Properties

Total filler amount (wt %)	CNT:CB	EMI SE (dB)	MFI (g/10 min)	Electrical conductivity (S m ⁻¹)
1	0:100	2.59 ± 0.98	25.58 ± 2.22	(2.41 ± 1.91) × 10 ^{-14a}
	25:75	5.39 ± 1.01	25.42 ± 1.23	(1.86 ± 1.23) × 10 ^{-12a}
	50:50	8.50 ± 0.40	24.28 ± 1.41	(2.00 ± 0.19) × 10 ^{-1b}
	75:25	11.92 ± 0.34	24.40 ± 1.35	(5.32 ± 2.56) × 10 ^{-1b}
	100:0	13.33 ± 0.53	21.29 ± 0.78	(1.50 ± 0.22) × 10 ^{0b}
3	0:100	5.45 ± 0.38	20.98 ± 1.88	(2.62 ± 0.84) × 10 ^{-2b}
	25:75	12.71 ± 0.49	14.64 ± 0.92	(5.47 ± 0.55) × 10 ^{0b}
	50:50	23.77 ± 0.29	12.10 ± 0.93	(1.17 ± 0.004) × 10 ^{1b}
	75:25	29.37 ± 0.19	10.06 ± 1.06	(2.99 ± 0.001) × 10 ^{1b}
	100:0	31.82 ± 0.26	6.89 ± 0.73	(3.16 ± 0.15) × 10 ^{1b}
5	0:100	8.47 ± 0.39	15.45 ± 2.09	(1.16 ± 0.06) × 10 ^{0b}
	25:75	23.14 ± 0.34	9.13 ± 0.49	(1.71 ± 0.19) × 10 ^{1b}
	50:50	33.11 ± 0.25	5.53 ± 0.28	(4.20 ± 0.06) × 10 ^{1b}
	75:25	40.10 ± 0.48	1.97 ± 0.07	(6.31 ± 0.31) × 10 ^{1b}
	100:0	45.32 ± 0.70	0.55 ± 0.04	(6.10 ± 0.08) × 10 ^{1b}

^aTwo-probe method.

^bFour-probe standard method.

composites displayed the same behavior: an increase in EMI SE and electrical conductivity, when the amount of CNT rises in comparison with the CB. However, the way those properties increase is somewhat different, while EMI SE presents an almost constant increase, the electrical conductivity of the composites shows a rapid increase when the amount of CNT exceeds a certain quantity, with the exception of the ABS/CNT:CB 5 wt % that shows small change in value of conductivity.

The difference in the properties behavior may be related to the fact that EMI SE is not only dependent of the composites electrical conductivity, but also the amount of filler incorporated. This occurs because the increase in electrical conductivity is mostly connected to the formation of a conductive path by the filler particles, and after that the values remain almost constant, however for EMI SE with the increase in filler content the interaction between emitted waves and the filler particles also increases, thus improving the SE. Since CNT seems to be the more effective filler in controlling the electrical properties of the hybrid composites, its increase also improves the EMI SE values. This behavior can be easily seen for the ABS/CNT:CB 5 wt % by considering the way EMI SE keeps increasing with the change in CNT amount but the electrical conductivity remains almost constant.

Additionally, EMI SE can be expressed as the sum of two different shielding mechanisms: reflection (SE_r) and absorption (SE_a) as reported in eq. (8). These mechanisms are determined by correlating the coefficient of reflectance, R , and the coefficient of transmittance, T , as shown in Eqs. (9) and (10).

$$\text{EMI SE} = SE_r + SE_a \quad (8)$$

$$SE_a = 10 \log \left(\frac{1-R}{T} \right) \quad (9)$$

$$SE_r = 10 \log \left(\frac{1}{1-R} \right) \quad (10)$$

The reflection mechanism occurs when the incident wave interacts with the electrons present at the materials surface, and depends mostly on the materials conductivity. The absorption mechanism happens when the wave penetrates the material and interacts with electrical dipoles present inside the material, and is associated to not only the electrical conductivity, but also the amount and distribution of filler in the matrix. For all composites, the main shielding mechanism was the absorption (Figure 11). The reflection contribution, besides being smaller than the absorption mechanism, shows less variation between the composites, both among the ones with the same amount of total filler, and between the composites with different total weight percentage. For example, if we take the 3 wt % composite [Figure 11(b)], the reflection mechanism contribution goes from 2.70 dB for 25:75 (CNT:CB) to 4.91 dB for 75:25, while the absorption goes from 10.01 dB to 23.99 dB, respectively. And if we compare the 50:50 for the 3 and 5 wt % composites, the reflection goes from 4.14 to 5.66 dB and the absorption goes from 18.67 to 27.45 dB, respectively. It is important to emphasize that the CNT have greater influence in both mechanisms, mostly due to the higher aspect ratio and tendency to create tridimensional conductive network.

Similarly to the binaries composites, the MFI value of the hybrid composites decreases with filler content (Figure 12). In addition, CNT showed a strong influence on this property resulting in the decrease of MFI with the increase of this filler fraction, for the same total amount of filler. For the ABS/CNT:CB with 3 wt % total filler [Figure 12(b)] the MFI decreases from 15 g/10 min (25:75) to 10 g/10 min (75:25), for the ABS/CNT:CB with 5 wt % total filler [Figure 12(c)] the change was even greater going from 9 g/10 min to 2 g/10 min when the fraction of CNT grew from 25% to 75%.

The materials properties are summarized in Table II. Comparing the values from the hybrid composites, it can be seen that for the same EMI SE different values of MFI can be obtained by changing the total amount of filler content and the fraction between the CNT and CB. Amongst the attained properties the one showed by ABS/CNT:CB with 3 wt % total filler content and fraction of 50:50 presents a good combination of EMI SE and MFI, 23.77 dB and 12.10 g/10 min, respectively. Also the ABS/CNT:CB with 3 wt % (75:25) shows a higher EMI SE, 29.37 dB, without decreasing to much the MFI.

CONCLUSIONS

The correlation between filler content, EMI SE, and MFI of ABS/CB, ABS/CNT, and ABS/CNT:CB hybrids was analyzed in this study. As expected, the increase of filler content resulted in the raise of electrical conductivity and EMI SE, but also the decrease of MFI value. The electrical conductivity of composites with 15 wt % increases by about 16 orders of magnitude in comparison with neat ABS. ABS/CNT showed the desired level of EMI SE, 20 dB, with a filler amount of less than 3 wt % while for ABS/CB an amount as high as 15 wt % of CB is required to reach this value. On the other hand, for 5 wt % ABS/CNT showed a MFI of 0.55 g/10 min while ABS/CB presented a value of 15.45 g/10 min. DMTA analysis indicates that, for the systems studied, the filler was presented in both phases of the matrix, though showed stronger influence to the butadiene phase. Through the hybrid composite of ABS with 1.5 wt % of CNT and 1.5 wt % of CB it was possible to obtain an EMI SE of 23.77 dB and a MFI of 12 g/10 min showing the great potential of this material for applications in which electromagnetic shielding must be accompanied by easy processing. In addition, with the hybrid composites it is possible to reduce the total cost of these materials, since some of CNTs could be replaced by CB. Finally, the values of EMI and electrical conductivity presented in this work opens the possibility of employing these materials not only on electromagnetic shielding applications, although this is the main objective of this work, but also for applications such as antistatic coatings, sensors, bipolar plates (for fuel cells), microelectronics, and others.

ACKNOWLEDGMENTS

The authors gratefully acknowledge the financial support of the Conselho Nacional de Desenvolvimento Científico e Tecnológico (CNPq), the Coordenação de Aperfeiçoamento de Pessoal de Ensino Superior (CAPES), Fundação de Amparo à Pesquisa e Inovação do Estado de Santa Catarina (FAPESC), and the Central Electron Microscopy Laboratory of Universidade Federal de Santa Catarina (LCME-UFSC) for the FEG-SEM images.

REFERENCES

1. Ramoa, S. D. A. S.; Barra, G. M. O.; Oliveira, R. V. B.; de Oliveira, M. G.; Cossad, M.; Soares, B. G. *Polym. Int.* **2013**, *62*, 1477.
2. Kuester, S.; Demarquette, N. R.; Ferreira, J. C.; Soares, B. G.; Barra, G. M. O. *Eur. Polym. J.* **2017**, *88*, 328.
3. Kuester, S.; Merlini, C.; Barra, G. M. O.; Ferreira, J. C.; Lucas, A.; de Souza, A. C.; Soares, B. G. *Compos. Part B: Eng.* **2016**, *84*, 236.
4. Al-Saleh, M. H.; Saadeh, W. H.; Sundararaj, U. *Carbon* **2013**, *60*, 146.
5. Al-Saleh, M. H. *Synth. Met.* **2016**, *217*, 322.
6. Sachdev, V. K.; Sudeshna, B.; Kamlesh, P.; Surender, K. S.; Navin, C. M.; Ram, P. T. *J. Appl. Polym. Sci.* **2014**, *131*. DOI: 10.1002/app.40201.
7. Mohd Radzuan, N. A.; Sulong, A. B.; Sahari, J. *Int. J. Hydrogen Energ.* **2017**, *42*, 9262.
8. Alig, I.; Skipa, T.; Lellinger, D.; Pötschke, P. *Polymer* **2008**, *49*, 3524.
9. Al-Saleh, M. H. *Synth. Met.* **2015**, *205*, 78.
10. Burmistrov, I.; Gorshkov, N.; Ilinykh, I.; Muratov, D.; Kolesnikov, E.; Anshin, S.; Mazov, I.; Issi, J.-P.; Kusnezov, D. *Compos. Sci. Technol.* **2016**, *129*, 79.
11. Al-Saleh, M. H. *Synth. Met.* **2015**, *209*, 41.
12. Szeluga, U.; Kumanek, B.; Trzebicka, B. *Compos. Part A: Appl. Sci. Manuf.* **2015**, *73*, 204.
13. Sharma, S. K.; Gupta, V.; Tandon, R. P.; Sachdev, V. K. *RSC Adv.* **2016**, *6*, 18257.
14. Wu, D.; Lv, Q.; Feng, S.; Chen, J.; Chen, Y.; Qiu, Y.; Yao, X. *Carbon* **2015**, *95*, 380.
15. Chen, J.; Du, X.-C.; Zhang, W.-B.; Yang, J.-H.; Zhang, N.; Huang, T.; Wang, Y. *Compos. Sci. Technol.* **2013**, *81*, 1.
16. Bauhofer, W.; Kovacs, J. Z. *Compos. Sci. Technol.* **2009**, *69*, 1486.
17. Jyoti, J.; Basu, S.; Singh, B. P.; Dhakate, S. R. *Compos. Part B: Eng.* **2015**, *83*, 58.
18. Al-Saleh, M. H.; Saadeh, W. H. *Mater. Des.* **2013**, *52*, 1071.
19. Socher, R.; Krause, B.; Boldt, R.; Hermasch, S.; Wursche, R.; Pötschke, P. *Compos. Sci. Technol.* **2011**, *71*, 306.
20. Menzer, K.; Krause, B.; Boldt, R.; Kretschmar, B.; Weidisch, R.; Pötschke, P. *Compos. Sci. Technol.* **2011**, *71*, 1936.
21. Kuester, S.; Barra, G. M. O.; Ferreira, J. C.; Soares, B. G.; Demarquette, N. R. *Eur. Polym. J.* **2016**, *77*, 43.
22. Ram, R.; Rahaman, M.; Khastgir, D. *Compos. Part A: Appl. Sci. Manuf.* **2015**, *69*, 30.
23. Socher, R.; Krause, B.; Hermasch, S.; Wursche, R.; Pötschke, P. *Compos. Sci. Technol.* **2011**, *71*, 1053.
24. Pan, Y.; Liu, X.; Hao, X.; Starý, Z.; Schubert, D. W. *Eur. Polym. J.* **2016**, *78*, 106.
25. Al-Saleh, M. H.; Sundararaj, U. *J. Polym. Sci. Part B: Polym. Phys.* **2012**, *50*, 1356.
26. Leyva, M. E.; Barra, G. M. O.; Moreira, A. C. F.; Soares, B. G.; Khastgir, D. *J. Polym. Sci. Part B: Polym. Phys.* **2003**, *41*, 2983.
27. Muller, D.; Garcia, M.; Salmoria, G. V.; Pires, A. T. N.; Paniago, R.; Barra, G. M. O. *J. Appl. Polym. Sci.* **2011**, *120*, 351.
28. Ornaghi, H. L.; Bolner, A. S.; Fiorio, R.; Zattera, A. J.; Amico, S. C. *J. Appl. Polym. Sci.* **2010**, *118*, 887.